Design of IIR fullband differentiators using parallel all-pass structure

Goran Stančić[a], Ivan Krstić[b,*], Miloš Živković[a]

[a] University of Niš, Faculty of Electronic Engineering, 18000 Niš, Serbia
[b] University of Priština, Faculty of Technical Sciences, 38220 Kosovska Mitrovica, Serbia

Abstract

A new approach for the design of recursive fullband digital differentiators using parallel all-pass structure is discussed in this paper. While magnitude response of designed fullband differentiator approximates the ideal one in the weighted Chebyshev sense, its phase response is a nearly-linear function of frequency at low frequencies. The low-pass differentiators, presented in this paper, are obtained by cascading the proposed recursive fullband differentiators with the corresponding low-pass filters. The phase response linearity error of such low-pass differentiators is shown to be primarily affected by the phase response nonlinearity of the utilized low-pass filter. A comparison with some of the existing fullband and low-pass differentiators shows that proposed differentiators require less multiplications, while their phase and magnitude responses are either better or slightly worse than those of existing differentiators.

Keywords: all-pass digital filter, parallel connection, weighted Chebyshev approximation, fullband differentiator, low-pass differentiator

1. Introduction

Digital fullband differentiators, needed in a wide range of digital signal processing applications [1, 2, 3, 4, 5] where the time derivative of input signal needs to be computed, can be designed either as an infinite impulse response (IIR) [6, 7, 8, 9, 10, 11, 12, 13, 14, 15, 16, 17, 18, 19, 20] or finite impulse response filters [21, 22, 23]. While the order of the IIR fullband differentiator is significantly lower compared to its finite impulse response filter counterpart, the perfectly linear phase response of IIR fullband differentiator cannot be achieved. On the other hand, this is not an issue in most practical applications if obtained phase response is nearly-linear function of frequency.

There are several approaches to the IIR fullband differentiator design. Conventional approach to the IIR differentiator design is based on inversion of the IIR integrator transfer function followed by reflection of the unstable poles inside the unit circle and compensation of the amplitude [6, 7, 8, 9]. In other words, conventional approach reduces to IIR integrator design problem. Starting point of design methods of the second approach is the IIR differentiator transfer function, obtained either by conventional approach or by any other design method, which is than optimized utilizing classical [10] or evolutionary [10, 16] optimization techniques. Methods of the third approach determine the unknown coefficients of the recursive transfer function such that some objective function is minimized. Design method presented in [12] formulates the IIR fullband differentiators' design problem as convex constrained optimization problem in unknown zeros' and poles' radiuses and phase angles, such that its solution minimizes the group delay-deviation under the constraint that maximum magnitude response error is below some prescribed value. Coefficients of the direct form differentiators' coefficients are determined by minimizing the L_2 norm of the magnitude response error by means of metaheuristic optimization techniques in [8, 14, 17], and by iterative quadratic

*Corresponding author
Email addresses: goran.stancic@elfak.ni.ac.rs (Goran Stančić), ivan.krstic@pr.ac.rs (Ivan Krstić), miskoz@elfak.rs (Miloš Živković)

programming approach in [18]. On the other hand, a noniterative method presented in [20] formulates the fullband differentiators' design problem as quadratic programming problem such that the magnitude and phase response specifications are simultaneously approximated. Another method of the third approach is given in [15] where coefficients of the lattice wave digital filter representation of the third and the fifth order fullband differentiators are determined by minimizing the L_1 norm error using the metaheuristic optimization technique.

In this paper, a new approach for the design of IIR fullband digital differentiators using parallel all-pass structure is presented. Magnitude response of obtained fullband differentiators approximate the ideal one in the weighted Chebyshev sense. On the other hand, although phase response linearity of proposed IIR fullband differentiators cannot be controlled, it is a nearly-linear function of frequency at low frequencies. Thus, phase response linearity of low-pass differentiator, obtained by cascading proposed IIR fullband differentiator with the corresponding low-pass filter, is primarily affected by the phase response linearity of the utilized low-pass filter. To the best of our knowledge, except differentiators presented in [15], design of IIR fullband differentiators using parallel all-pass structure does not appear to be considered in the existing literature.

The rest of the paper is structured as follows. In Sec. 2, the problem formulation of an all-pass based IIR fullband differentiator with a magnitude response approximating the ideal one in weighted Chebyshev sense is presented. The proposed IIR fullband differentiator design method is discussed in Sec. 3, while design examples and comparison with some of the existing fullband and low-pass differentiators (the proposed low-pass differentiators are obtained by cascading proposed fullband differentiators with the corresponding low-pass filters) are presented in Sec. 4. Finally, concluding remarks are given in Sec. 5.

2. Problem formulation

Transfer function of the IIR fullband differentiators, whose design is considered in this paper, is assumed to be of the following form

$$H(z) = \frac{\pi}{2}\left[A_N(z) - z^{-(N-1)}\right], \tag{1}$$

as depicted in Fig. 1, where $A_N(z)$ is the transfer function of Nth order stable all-pass filter with single poles

$$A_N(z) = z^{-N}\frac{1+\sum_{i=1}^{N} a_i z^{i}}{1+\sum_{i=1}^{N} a_i z^{-i}}. \tag{2}$$

Substituting $z = e^{j\omega}$ in Eq. 1, followed by some mathematical manipulations, magnitude and phase re-

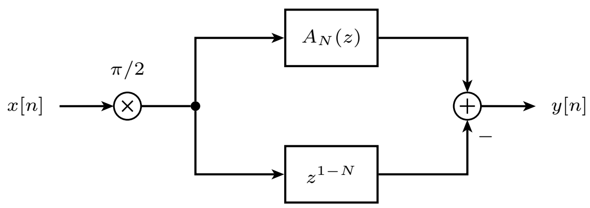

Figure 1: Fullband differentiator realized using parallel all-pass structure.

sponses of the proposed fullband differentiator are obtained as

$$\left|H\left(e^{j\omega}\right)\right| = \pi\left|\sin\frac{\phi(\omega)+(N-1)\omega}{2}\right|, \tag{3}$$

$$\varphi_H(\omega) = \frac{\phi(\omega)-(N-1)\omega+\pi}{2}, \tag{4}$$

where $\phi(\omega)$ denotes phase response of the all-pass filter $A_N(z)$, which can be obtained from Eq. 2 as

$$\phi(\omega) = -N\omega + 2\arctan\frac{\sum_{i=1}^{N} a_i \sin(i\omega)}{1 + \sum_{i=1}^{N} a_i \cos(i\omega)}. \tag{5}$$

Obviously magnitude response given by Eq. 3 will approximate the magnitude response of an ideal fullband differentiator

$$\left|H_{id}\left(e^{j\omega}\right)\right| = \omega, \tag{6}$$

if the phase response of the corresponding all-pass filter $A_N(z)$ approximates

$$\phi'(\omega) = -(N-1)\omega - 2\arcsin\frac{\omega}{\pi}, \tag{7}$$

for $\omega \in [0, \pi]$. Since phase response $\phi(\omega)$ of the stable Nth order all-pass filter $A_N(z)$ with real coefficients satisfies $\phi(0) = \phi'(0) = 0$ and $\phi(\pi) = \phi'(\pi) = -N\pi$, it can be concluded that $\left|H\left(e^{j0}\right)\right| = \left|H_{id}\left(e^{j0}\right)\right| = 0$ and $\left|H\left(e^{j\pi}\right)\right| = \left|H_{id}\left(e^{j\pi}\right)\right| = \pi$. Ideal phase response $\phi'(\omega)$ of the second order all-pass filter $A_2(z)$, characterizing the third order fullband differentiator, is shown in Fig. 2.

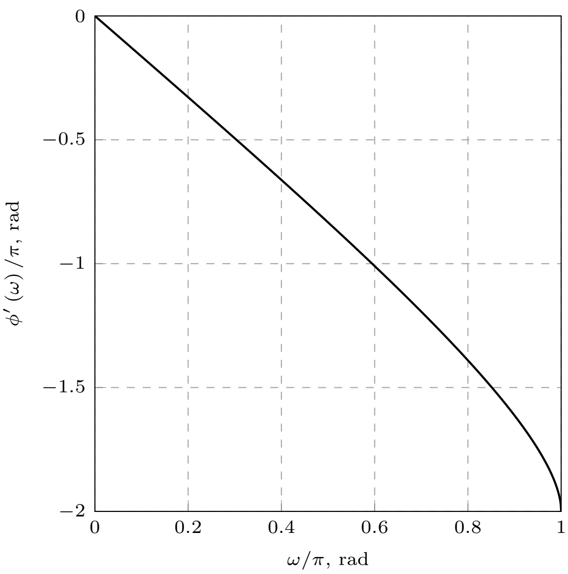

Figure 2: Ideal phase response of the all-pass filter $A_2(z)$ characterizing the 3rd order IIR fullband differentiator.

By rewriting Eq. 3 using Eq. 7 as

$$\left|H\left(e^{j\omega}\right)\right| = \pi\left|\sin\left(\arcsin\frac{\omega}{\pi} - \frac{\phi(\omega) - \phi'(\omega)}{2}\right)\right|, \tag{8}$$

and assuming that the magnitude response of the fullband differentiator approximates ideal magnitude response given by Eq. 6 in the weighted Chebyshev sense, that is

$$\varepsilon_{mag}(\omega_k) = \left|H\left(e^{j\omega_k}\right)\right| - \omega_k = (-1)^{k+p}\frac{\delta}{W_k}, \tag{9}$$

for $k = 1, 2, \ldots, N+1$, where W_k is the weighting factor associated to the kth extremal value of the magnitude error function $\varepsilon_{mag}(\omega)$, $0 < \omega_1 < \omega_2 < \ldots < \omega_{N+1} < \pi$ are frequency points where those extremal values occur, parameter $p \in \{0, 1\}$ determines whether maximum ($p = 1$) or minimum ($p = 0$)

of the magnitude error function occurs at frequency $\omega = \omega_1$, while $\delta > 0$ is the corresponding weighted Chebyshev norm, it follows that

$$\pi \left| \sin \left(\arcsin \frac{\omega_k}{\pi} - \frac{\phi(\omega_k) - \phi'(\omega_k)}{2} \right) \right| = \omega_k + (-1)^{k+p} \frac{\delta}{W_k}, \tag{10}$$

for $k = 1, 2, \ldots, N+1$. Adopting a reasonable assumption that the all-pass filter's phase response approximation error

$$\varepsilon_{ph}(\omega) = \phi(\omega) - \phi'(\omega), \tag{11}$$

for $\omega = \omega_1$ satisfies inequality

$$|\varepsilon_{ph}(\omega_1)| < \arcsin \frac{\omega_1}{\pi}, \tag{12}$$

Eq. 10 reduces to

$$\pi \sin \left(\arcsin \frac{\omega_k}{\pi} - \frac{\phi(\omega_k) - \phi'(\omega_k)}{2} \right) = \omega_k + (-1)^{k+p} \frac{\delta}{W_k} \tag{13}$$

or equivalently

$$-\pi \sin \frac{\phi(\omega_k) + (N-1)\omega_k}{2} = \omega_k + (-1)^{k+p} \frac{\delta}{W_k}, \tag{14}$$

for $k = 1, 2, \ldots, N+1$. Note that for $p = 0$, $\omega_1 \geq \delta$, while for $N + p + 1$ even, $\omega_{N+1} \leq \pi - \delta$. In the case of equiripple magnitude response of the IIR fullband differentiator ($W_k = 1$ for $k = 1, 2, \ldots, N+1$), the upper and lower envelopes of the phase response approximation error $\varepsilon_{ph}(\omega)$ of the corresponding all-pass filter $A_N(z)$ can be determined from Eq. 13 as follows

$$\begin{aligned} U_{\varepsilon_{ph}}(\omega) &= 2\left(\arcsin \tfrac{\omega}{\pi} - \arcsin \tfrac{-\delta+\omega}{\pi}\right), \\ L_{\varepsilon_{ph}}(\omega) &= 2\left(\arcsin \tfrac{\omega}{\pi} - \arcsin \tfrac{\delta+\omega}{\pi}\right), \end{aligned} \tag{15}$$

respectively. Plots of those envelopes for various values of the Chebyshev norm δ and $\omega \in [\delta, \pi - \delta]$ are given in Fig. 3. As expected, with δ decreasing phase error envelopes becomes closer to 0, that is phase response approximation error becomes smaller. Another conclusion that can be drawn from Fig. 3 is that the phase response of the proposed fullband differentiator (Eq. 4) with equiripple magnitude response cannot be equiripple.

Since the ideal phase response (note that term "ideal" means that the magnitude response of the proposed IIR fullband differentiator is linear, but not its phase response) of the proposed IIR fullband differentiator approximately equals

$$-(N-1)\omega - \frac{\omega}{\pi} + \frac{\pi}{2},$$

for ω small, Eqs. 7 and 4, which is linear function of frequency, low-pass differentiators with nearly-linear phase can be obtained by a cascading approach. Therefore, the phase response linearity error of such IIR low-pass differentiators is primarily affected by the phase response linearity error of the utilized low-pass filters.

In the following section, the iterative procedure for the determination of the unknown all-pass filter coefficients' vector

$$\mathbf{a} = [a_1, a_2, \ldots, a_N]^T, \tag{16}$$

such that the obtained magnitude response of the IIR fullband differentiator approximates the ideal one in the weighted Chebyshev sense is discussed. Determination of the initial solution vector $\mathbf{a}^{(0)}$ such that $\varepsilon_{mag}\left(\omega, \mathbf{a}^{(0)}\right)$ exhibit $N+1$ sign-alternating extremal values will be treated separately. Notation $H(z, \mathbf{W})$ will be used in the following text whenever the dependence of the IIR fullband differentiator transfer function on the weighting factors

$$\mathbf{W} = [W_1, W_2, \ldots, W_{N+1}], \tag{17}$$

needs to be emphasized.

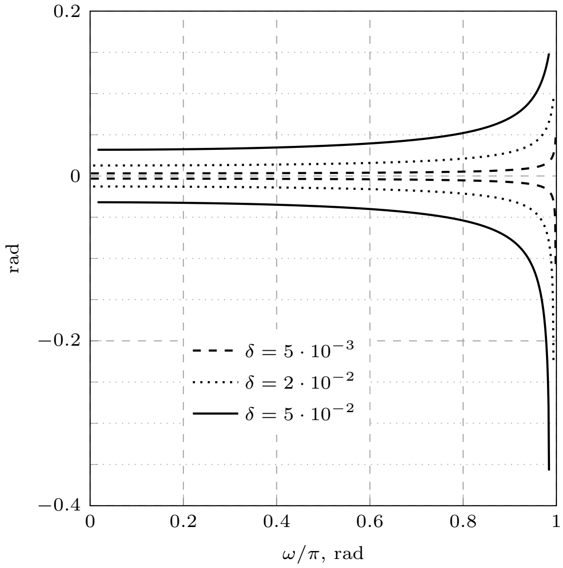

Figure 3: Envelopes of the phase error function $\varepsilon_{ph}(\omega)$ for various values of the Chebyshev norm δ, $\omega \in [\delta, \pi - \delta]$ and $W_k = 1$, for $k = 1, 2, \ldots, N+1$.

3. Proposed design

In order to obtain weighted Chebyshev approximation of the fullband differentiator's magnitude response, Eq. 14, iterative approach is proposed. In every iteration $t \geq 1$ of the algorithm, coefficients' vector $\mathbf{a}^{(t)}$ and the value of the parameter $\delta^{(t)}$ are obtained by means of previously determined vector $\mathbf{a}^{(t-1)}$ and the parameter $\delta^{(t-1)}$. Mentioned update process is performed by solving approximately the following system of equations (note Eq. 14):

$$\sin\frac{\phi\left(\omega_k^{(t-1)},\, \mathbf{a}^{(t)}\right) + (N-1)\,\omega_k^{(t-1)}}{2} = -\frac{1}{\pi}\left[\omega_k^{(t-1)} + (-1)^{k+p}\,\frac{\delta^{(t)}}{W_k}\right], \tag{18}$$

for $k = 1, 2, \ldots, N+1$, where $\omega_k^{(t-1)}$ is the frequency position of the kth extremum point of the magnitude error function $\varepsilon_{mag}\left(\omega,\, \mathbf{a}^{(t-1)}\right)$. Namely, since Eq. 18 is nonlinear in an unknown coefficients vector $\mathbf{a}^{(t)}$, its left-hand side is linearized about $\mathbf{a}^{(t-1)}$ by replacing it by its first order Taylor expansion

$$\sin\frac{\phi\left(\omega_k^{(t-1)},\, \mathbf{a}^{(t-1)}\right) + (N-1)\,\omega_k^{(t-1)}}{2} + \frac{1}{2}\cos\frac{\phi\left(\omega_k^{(t-1)},\, \mathbf{a}^{(t-1)}\right) + (N-1)\,\omega_k^{(t-1)}}{2}\sum_{i=1}^{N}\frac{\partial\phi\left(\omega_k^{(t-1)},\, \mathbf{a}^{(t-1)}\right)}{\partial a_i}\Delta a_i, \tag{19}$$

for $k = 1, 2, \ldots, N+1$, where partial derivatives can be determined from Eq. 5 as

$$\frac{\partial\phi\left(\omega_k^{(t-1)},\, \mathbf{a}^{(t-1)}\right)}{\partial a_i} = 2\frac{\sin\left(i\omega_k^{(t-1)}\right) + \sum_{n=1}^{N} a_n^{(t-1)}\sin\left(\omega_k^{(t-1)}(i-n)\right)}{\left(1 + \sum_{n=1}^{N} a_n^{(t-1)}\cos\left(n\omega_k^{(t-1)}\right)\right)^2 + \left(\sum_{n=1}^{N} a_n^{(t-1)}\sin\left(n\omega_k^{(t-1)}\right)\right)^2}. \tag{20}$$

In this way, linearized form of Eq. 18 can be rewritten in matrix notation as

$$\mathbf{\Psi}^{(t-1)} \cdot \left[\begin{array}{c} \Delta\mathbf{a}^{(t)} = \mathbf{a}^{(t)} - \mathbf{a}^{(t-1)} \\ \Delta\delta^{(t)} = \delta^{(t)} - \delta^{(t-1)} \end{array}\right] = \boldsymbol{\lambda}^{(t-1)}, \tag{21}$$

where $\mathbf{\Psi}^{(t-1)} = \left[\psi_{ki}^{(t-1)}\right]$ is the $(N+1)\times(N+1)$ square matrix, while $\boldsymbol{\lambda}^{(t-1)} = \left[\lambda_k^{(t-1)}\right]$ is the $(N+1)\times 1$ column vector, with elements

$$\psi_{ki}^{(t-1)} = \begin{cases} \frac{\pi}{2}\frac{\partial\phi\left(\omega_k^{(t-1)},\,\mathbf{a}^{(t-1)}\right)}{\partial a_i}\cos\frac{\phi\left(\omega_k^{(t-1)},\,\mathbf{a}^{(t-1)}\right)+(N-1)\omega_k^{(t-1)}}{2}, & 1\le i\le N \\ \frac{(-1)^{k+p}}{W_k}, & i=N+1 \end{cases}, \tag{22}$$

$$\lambda_k^{(t-1)} = -\omega_k^{(t-1)} + (-1)^{k+p+1}\frac{\delta^{(t-1)}}{W_k} - \pi\sin\frac{\phi\left(\omega_k^{(t-1)},\,\mathbf{a}^{(t-1)}\right)+(N-1)\,\omega_k^{(t-1)}}{2}. \tag{23}$$

Based on the above discussion and assuming $\mathbf{a}^{(t-1)}$ and $\delta^{(t-1)}$ known, approximate solution for the unknowns $\delta^{(t)}$ and $\mathbf{a}^{(t)}$ can be obtained by solving the system of linear equations given by Eq. 21. On the other hand, the obtained solution does not guarantee that extremal values of the IIR fullband differentiator's magnitude response error function occur at frequencies $\omega_k^{(t-1)}$, $k=1,\,2,\,\ldots,\,N+1$. Hence, we propose the following exchange algorithm for the IIR fullband differentiator design:

0. $t=0$. Set $\delta^{(0)}$ to 10^{-4}.
1. Based on the known coefficients' vector $\mathbf{a}^{(t)}$ determine the set of frequencies $\omega_1^{(t)} < \omega_2^{(t)} < \ldots < \omega_{N+1}^{(t)}$ where sign-alternating extremal values of $\varepsilon_{mag}\left(\omega,\,\mathbf{a}^{(t)}\right)$ occur.
2. $t=t+1$. Determine $\Delta\mathbf{a}^{(t)}$ and $\Delta\delta^{(t)}$ using Eq. 21 as

$$\begin{bmatrix}\Delta\mathbf{a}^{(t)}\\ \Delta\delta^{(t)}\end{bmatrix} = \left(\mathbf{\Psi}^{(t-1)}\right)^{-1}\cdot\boldsymbol{\lambda}^{(t-1)}. \tag{24}$$

3. If $\max\left\{\left|\Delta\mathbf{a}^{(t)}\right|,\,\left|\Delta\delta^{(t)}\right|\right\} \le \Delta_{tol}$, where Δ_{tol} is the prescribed tolerance, jump to the next step, otherwise proceed from the step 1.
4. The end of the algorithm. Unknown coefficients' vector $\mathbf{a}$ equals $\mathbf{a}^{(t)}$, while weighted Chebyshev norm δ equals $\delta^{(t)}$.

3.1. Determination of the initial solution

Since the initial solution for the all-pass filter's coefficients $\mathbf{a}^{(0)}$ should be such that the magnitude response error function $\varepsilon_{mag}\left(\omega,\,\mathbf{a}^{(0)}\right)$ has $N+1$ sign-alternating extremal points, it will be determined by setting the all-pass filter's phase response error function $\varepsilon_{ph}\left(\omega,\,\mathbf{a}^{(0)}\right)$ to zero at N distinct equidistant frequency points:

$$\widetilde{\omega}_k = k\frac{\pi}{N+1}, \quad k=1,\,2,\,\ldots,\,N, \tag{25}$$

which is equivalent to

$$\phi\left(\widetilde{\omega}_k,\,\mathbf{a}^{(0)}\right) = \phi'\left(\widetilde{\omega}_k\right) = -\left(N-1\right)\widetilde{\omega}_k - 2\arcsin\frac{\widetilde{\omega}_k}{\pi}, \tag{26}$$

for $k=1,\,2,\,\ldots,\,N$.

As the phase response $\phi\left(\omega\right)$ of the all-pass filter $A_N\left(z\right)$ is related to its coefficients as

$$\sum_{i=1}^{N} a_i\sin\frac{\phi\left(\omega\right)+\left(N-2i\right)\omega}{2} = -\sin\frac{\phi\left(\omega\right)+N\omega}{2}, \tag{27}$$

which can be easily derived from Eq. 5, Eq. 26 can be rewritten as

$$\sum_{i=1}^{N} a_i^{(0)}\sin\left[\widetilde{\omega}_k\left(\frac{1}{2}-i\right) - \arcsin\frac{\widetilde{\omega}_k}{\pi}\right] = -\sin\left[\frac{\widetilde{\omega}_k}{2} - \arcsin\frac{\widetilde{\omega}_k}{\pi}\right], \tag{28}$$

for $k=1,\,2,\,\ldots,\,N$. Therefore, the solution for $\mathbf{a}^{(0)}$ can be determined using

$$\mathbf{a}^{(0)} = \mathbf{\Upsilon}^{-1}\boldsymbol{\gamma}, \tag{29}$$

where $\boldsymbol{\Upsilon} = [\upsilon_{ki}]$ is the $N \times N$ matrix, while $\boldsymbol{\gamma} = [\gamma_k]$ is the $N \times 1$ column vector such that

$$\upsilon_{ki} = \sin\left[\widetilde{\omega}_k \left(\frac{1}{2} - i\right) - \arcsin\frac{\widetilde{\omega}_k}{\pi}\right], \quad \gamma_k = -\sin\left[\frac{\widetilde{\omega}_k}{2} - \arcsin\frac{\widetilde{\omega}_k}{\pi}\right]. \tag{30}$$

Poles of the IIR fullband differentiator's transfer function that correspond to the initial solution coefficients' vector $\mathbf{a}^{(0)}$, for N from 2 to 6, are given in Tab. 1. As can be observed from Tab. 1, for every N from 2 to 6, one real pole is placed at the phase angle of π rad. Furthermore, since this is shown to be true for every N up to 100, it seems to be true for every N.

Table 1: Poles of the transfer function corresponding to the coefficients' vector $\mathbf{a}^{(0)}$, for N from 2 to 6.

N				
2	3	4	5	6
$0.394623 \cdot e^{j\pi}$	$0.477033 \cdot e^{j\pi}$	$0.536694 \cdot e^{j\pi}$	$0.582487 \cdot e^{j\pi}$	$0.619013 \cdot e^{j\pi}$
0.103535	$0.181456 \cdot e^{\pm j0.335530\pi}$	0.222670	$0.324552 \cdot e^{\pm j0.584852\pi}$	0.311111
		$0.257668 \cdot e^{\pm j0.491652\pi}$	$0.275037 \cdot e^{\pm j0.193385\pi}$	$0.381936 \cdot e^{\pm j0.647752\pi}$
				$0.325688 \cdot e^{\pm j0.321006\pi}$

All-pass filter's phase response error functions $\varepsilon_{ph}\left(\omega, \mathbf{a}^{(0)}\right)$ and corresponding fullband differentiator's magnitude response error functions $\varepsilon_{mag}\left(\omega, \mathbf{a}^{(0)}\right)$ are shown in Fig. 4. As expected, the proposed initial solution determination procedure results in fullband differentiator's magnitude error function and the all-pass filter's phase response error function having $N+1$ extremal values.

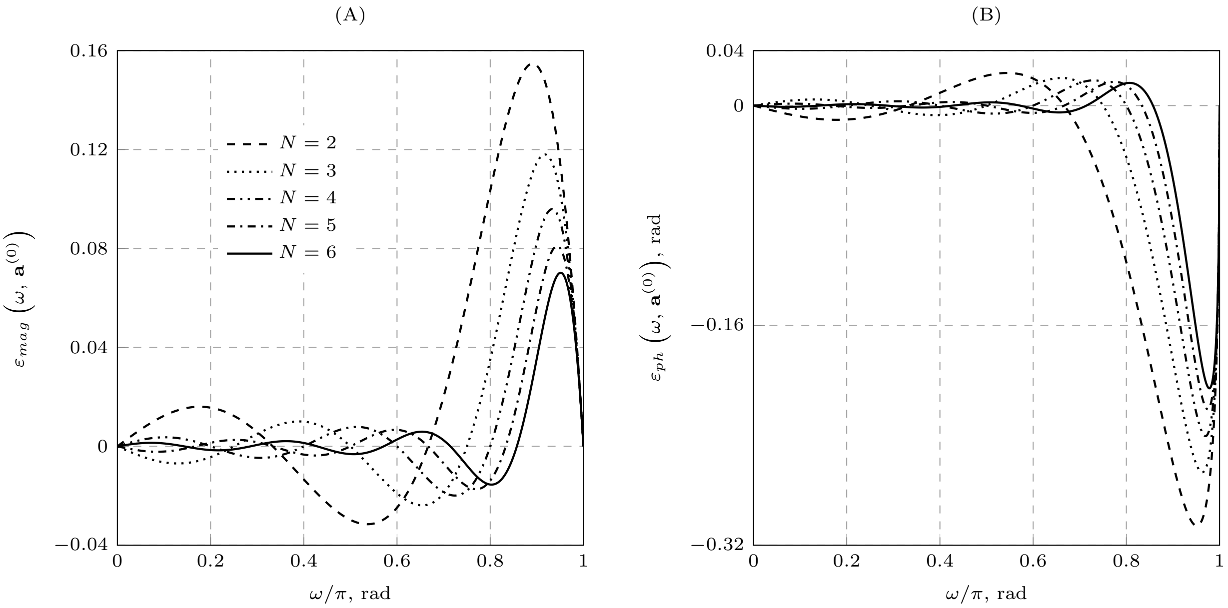

Figure 4: (A) Fullband differentiator's magnitude response error function $\varepsilon_{mag}\left(\omega, \mathbf{a}^{(0)}\right)$ and (B) corresponding all-pass filter's phase response error function $\varepsilon_{ph}\left(\omega, \mathbf{a}^{(0)}\right)$, for N from 2 to 6.

4. Design examples and comparison with existing fullband and low-pass differentiators

Design examples of the IIR fullband differentiators with equiripple magnitude responses ($W_1 = W_2 = \ldots = W_{N+1} = 1$), as well as the IIR low-pass differentiators obtained by cascading proposed fullband differentiators with the Chebyshev I low-pass filters having 0.1 dB ripple in the passband, are considered in this section. Mentioned choice of the low-pass filter type and its passband ripple value is adopted such that the comparison with the IIR low-pass differentiators presented in [24] is straightforward.

Let $G(z)$ denote the transfer function of the low-pass differentiator, which in our case equals

$$G(z) = H(z)\, Q_L(z), \tag{31}$$

where $Q_L(z)$ is the transfer function of the Lth order Chebyshev I low-pass filter having 0.1 dB passband ripple value. Average passband group delay of both fullband and low-pass differentiators can be expressed as

$$\overline{\tau} = \frac{\varphi(0) - \varphi(\omega_p)}{\omega_p}, \tag{32}$$

where ω_p is the passband edge frequency which in case of fullband differentiator equals π rad, while $\varphi(\omega)$ is the phase response of the differentiator

$$\varphi(\omega) = \begin{cases} \varphi_H(\omega) + \varphi_Q(\omega), & \omega_p < \pi \\ \varphi_H(\omega), & \omega_p = \pi \end{cases}, \tag{33}$$

and $\varphi_Q(\omega)$ is the phase response of the utilized low-pass filter. Employing Eq. 4 and the properties of the phase response of the stable all-pass filter $A_N(z)$ ($\phi(0) = 0$, $\phi(\pi) = \pi$), as well as the fact that $\varphi_Q(0) = 0$, average passband group delay of the proposed differentiators can be determined as

$$\overline{\tau} = \begin{cases} \frac{\pi - 2(\varphi_H(\omega_p) + \varphi_Q(\omega_p))}{2\omega_p}, & \omega_p < \pi \\ N - 0.5, & \omega_p = \pi \end{cases}. \tag{34}$$

As the means of comparison between IIR differentiators obtained using proposed and existing design methods, the phase response linearity error function defined as [12]

$$\xi_{ph}(\omega) = \varphi(\omega) - \left(\frac{\pi}{2} - \omega\overline{\tau}\right), \tag{35}$$

along with the absolute magnitude response error function

$$\xi_{mag}(\omega) = \begin{cases} \left|\left|G\left(e^{j\omega}\right)\right| - \omega\right|, & \omega_p < \pi \\ \left|\left|H\left(e^{j\omega}\right)\right| - \omega\right|, & \omega_p = \pi \end{cases}, \tag{36}$$

will be used. Clearly, the maximum value of $\xi_{mag}(\omega)$ in the passband when $\omega_p < \pi$ (that is when low-pass differentiators considered) can be decreased by suitable choice of the weighting factors W_k, $k = 1, 2, \ldots, N+1$, for the corresponding proposed IIR fullband differentiator design. Based on the previous equation, it can be concluded that the magnitude response error function of the obtained IIR low-pass differentiator is not necessarily equiripple.

4.1. IIR fullband differentiator with equiripple magnitude response

IIR fullband differentiators with equiripple magnitude responses ($W_k = 1$ for $k = 1, 2, \ldots, N+1$) characterized by the all-pass filters of order N from 1 to 40 were designed using the proposed method with Δ_{tol} equal to 10^{-10}. Required number of iterations for the algorithm to converge for each N from 1 to 40 is less than or equal to 6. Therefore, it can be concluded that the proposed algorithm exhibits fast convergence if weighting factors are equal to 1. Based on determined Chebyshev norms δ and assuming the following approximating function

$$\log_{10} N = C_1\delta^{-1} + C_2 \ln\delta + C_3, \tag{37}$$

unknown parameters C_1, C_2 and C_3 were determined using nonlinear regression

$$\begin{aligned} C_1 &= -0.000843923409228, \\ C_2 &= -0.536473372397133, \\ C_3 &= -0.898222004574358. \end{aligned} \tag{38}$$

In Fig. 5, the obtained Chebyshev norms (depicted with dots) are presented along with approximating function $N = 10^{C_1\delta^{-1}+C_2 \ln \delta + C_3}$ (solid line). As can be seen, the assumed function approximates the obtained Chebyshev norms well. Therefore, we propose the following inequality for estimating the required order of the all-pass filter characterizing IIR fullband differentiator such that its maximum magnitude response error is less than or equal to $\delta_{\max}$:

$$N \geq 10^{C_1\delta_{\max}^{-1}+C_2 \ln \delta_{\max} + C_3}. \tag{39}$$

Obtained fullband differentiator's magnitude and phase responses, for $N = 3$, 6, 8, are given in Fig. 6, while

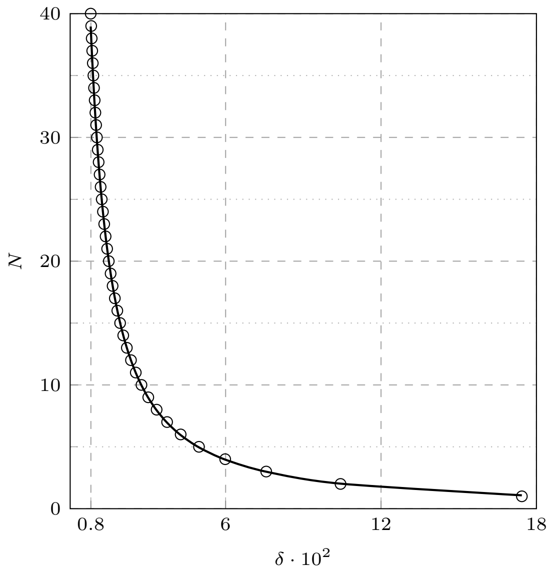

Figure 5: IIR fullband differentiator with equiripple magnitude response: Order of the all-pass filter N vs. Chebyshev norm δ.

the corresponding error functions are presented in Fig. 7. While the maximum of the fullband differentiator's magnitude response error decreases with the increase of the all-pass filter order, Fig. 7A, the improvement of the magnitude response is not followed by the improvement of the fullband differentiator's phase response, Fig. 7B, as expected having in mind Eqs. 7 and 4.

4.1.1. Comparison with existing IIR fullband differentiators

Proposed 3rd order IIR fullband differentiator with equiripple magnitude response is being compared to many existing IIR fullband differentiators of the same order. However, only results of comparison with the representative existing differentiators, that is those with better or comparable magnitude response and phase response linearity errors, are presented in the following text. On the other hand, proposed 5th order fullband differentiator is compared to only two differentiators of the same order that could be found in the existing literature. Since the overall order of the proposed IIR fullband differentiators equals $2N - 1$, Eq. 1, the order of the corresponding all-pass filter $A_N(z)$ equals 2 and 3 in case of the 3rd and 5th order fullband differentiator, respectively.

Magnitude and phase responses of the proposed and existing 3rd order IIR fullband differentiators from [15, 8, 10, 12] are presented in Fig. 8A and Fig. 8B, respectively. Corresponding magnitude and phase response error functions are given in Fig. 9. As can be seen on Fig. 9B, the proposed 3rd order IIR fullband differentiator with equiripple magnitude response exhibits lower phase response linearity error compared to the all-pass based differentiator from recently published paper [15]. However, the magnitude response error of the proposed differentiator is slightly higher. On the other hand, phase response linearity errors of the differentiators from [8, 10, 12] are lower compared to the phase linearity error of the proposed one, while

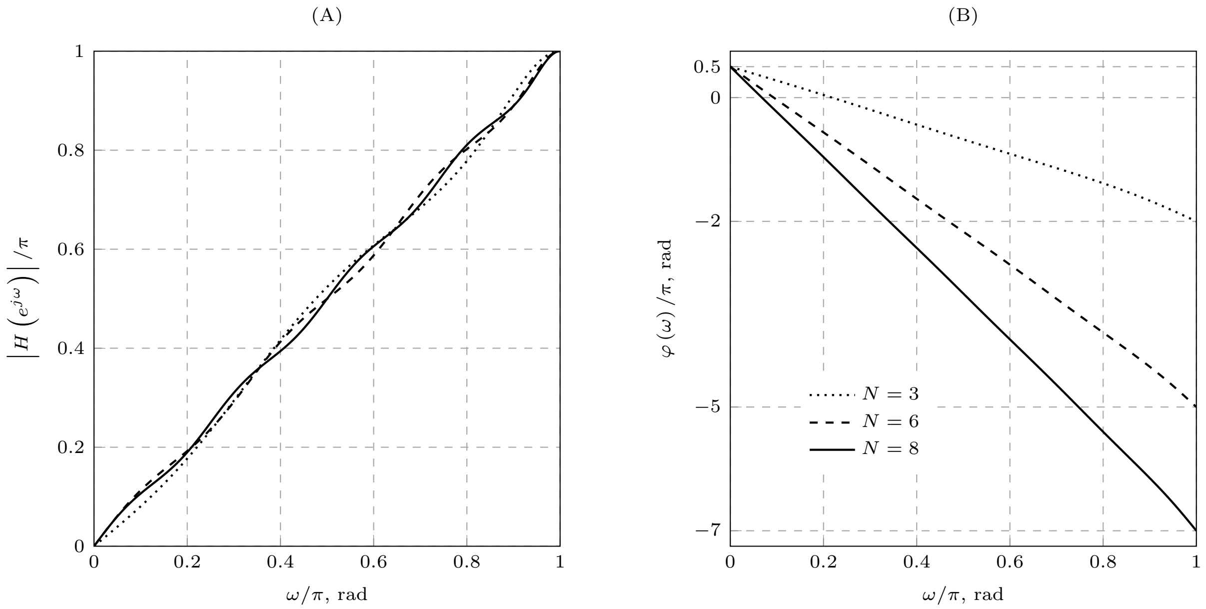

Figure 6: (A) Magnitude and (B) phase responses of the recursive fullband differentiator, for $N = 3$, 6, 8.

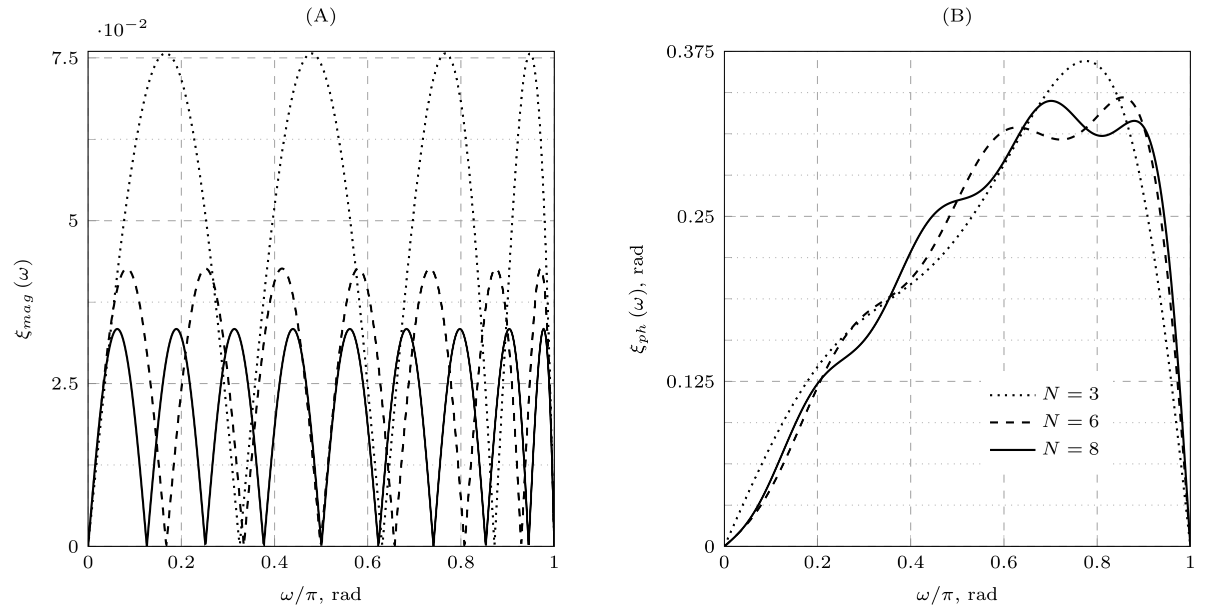

Figure 7: (A) Absolute magnitude response error function and (B) phase response linearity error function of the recursive fullband differentiator, for $N = 3$, 6, 8.

proposed differentiator exhibits lower magnitude response error at frequencies close to Nyquist frequency compared to differentiator from [8].

Magnitude and phase responses of the 5th order proposed and existing differentiators of the same order from [15, 13] are shown in Fig. 10A and Fig. 10B, respectively. Corresponding magnitude and phase response error functions are given in Fig. 11. As obvious from Figs. 10A and 11A, the proposed differentiator exhibits the highest magnitude response error compared to differentiators from [15, 13], while its phase response linearity error is by far the lowest, Figs. 10B and 11B.

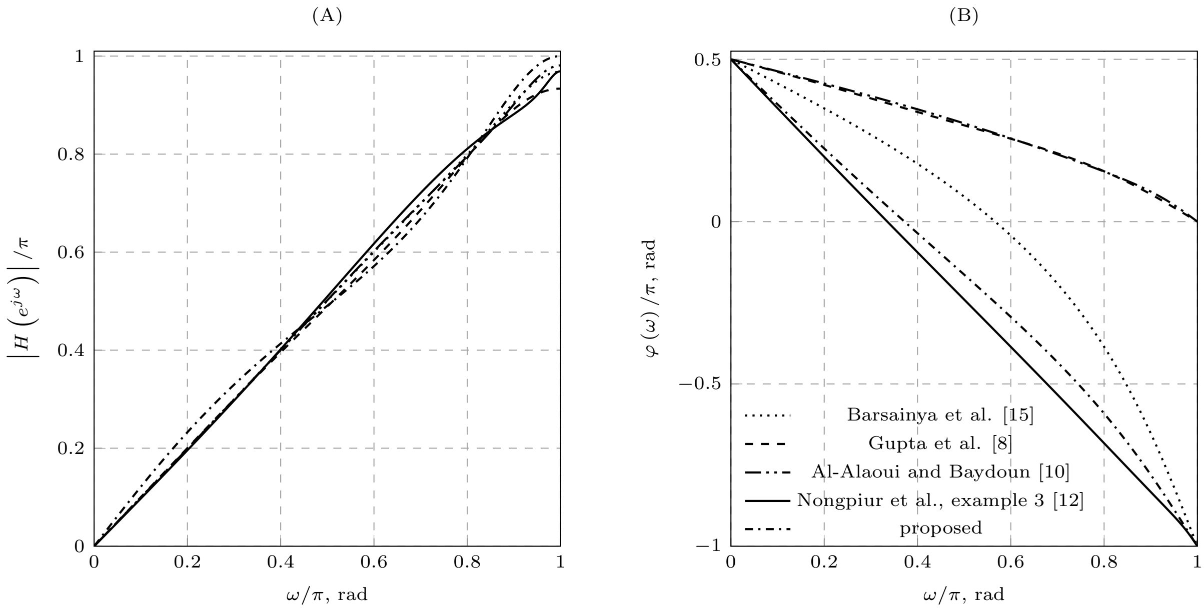

Figure 8: (A) Magnitude and (B) phase responses of the 3rd order proposed and existing recursive fullband differentiators.

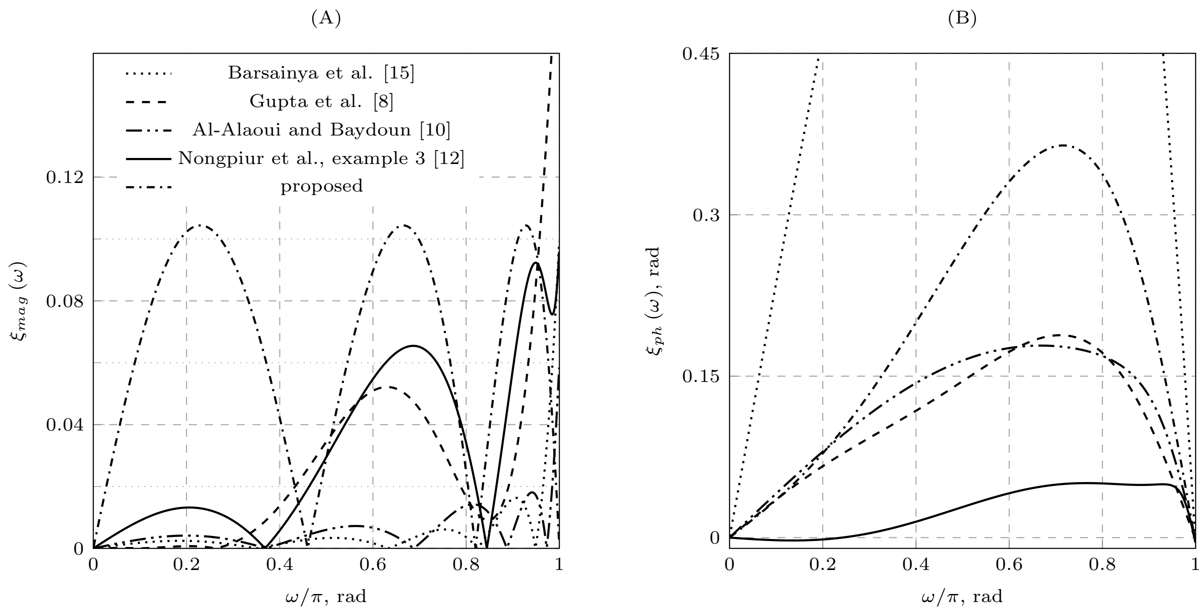

Figure 9: (A) Absolute magnitude response error function and (B) phase response linearity error function of the 3rd order proposed and existing recursive fullband differentiators.

Coefficients of the proposed and existing IIR fullband differentiators are given in Tab. 2, while needed number of multiplications required by those differentiators, maximum absolute magnitude response and phase response linearity errors are given in Tab. 3. Evidently, proposed design requires less multiplications compared to fullband differentiators from [15, 8, 10, 13].

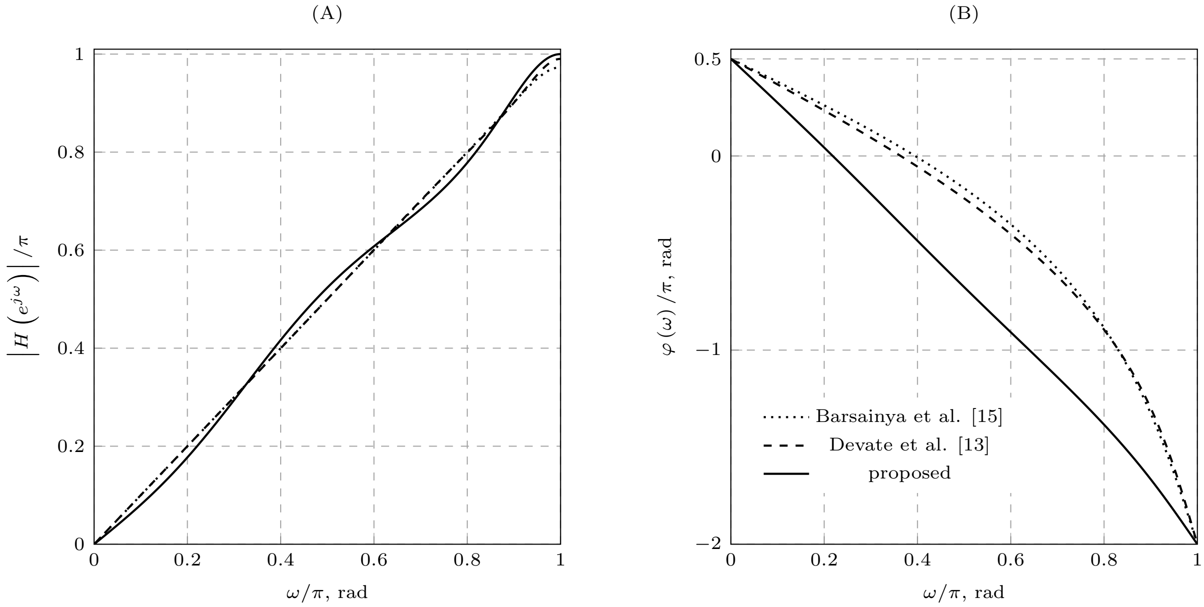

Figure 10: (A) Magnitude and (B) phase responses of the 5th order proposed and existing IIR fullband differentiators.

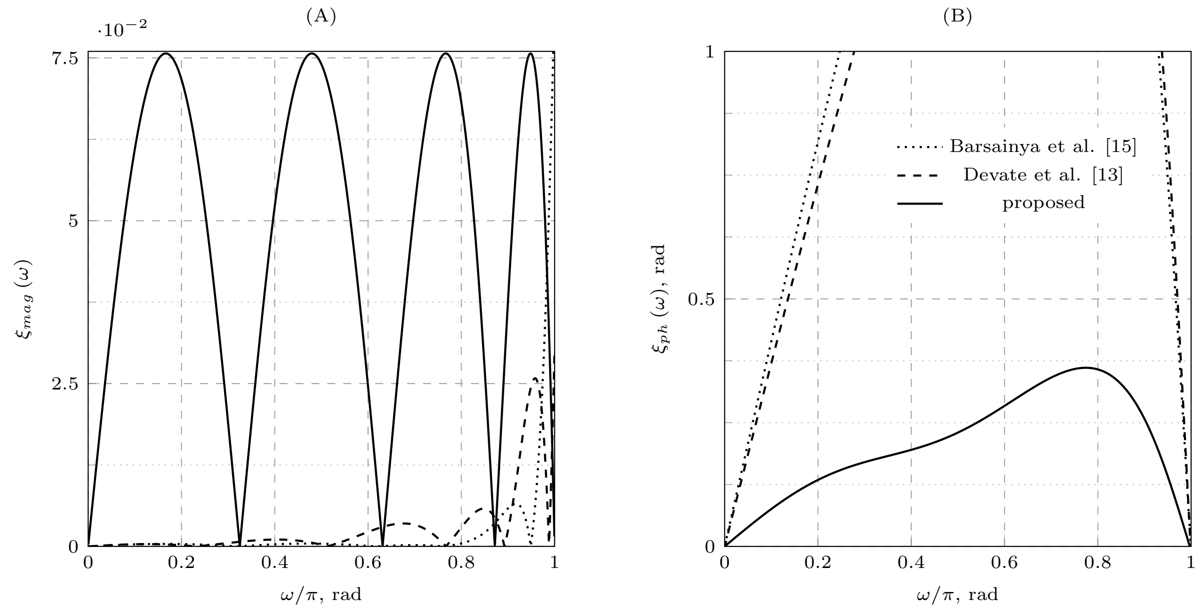

Figure 11: (A) Absolute magnitude response error function and (B) phase response linearity error function of the 5th order proposed and existing IIR fullband differentiators.

4.2. IIR low-pass differentiators

Magnitude and phase responses and the corresponding error functions of two low-pass differentiators obtained by cascading 5th order proposed fullband differentiators $H\left(z,\, \mathbf{W}^{(1)}\right)$ and $H\left(z,\, \mathbf{W}^{(2)}\right)$, where

$$\mathbf{W}^{(1)} = [1,\, 1,\, 1,\, 1]\,, \tag{40}$$

$$\mathbf{W}^{(2)} = [100,\, 100,\, 100,\, 1]\,, \tag{41}$$

Table 2: Coefficients of the proposed and existing recursive fullband differentiators.

Order	Reference	Numerator coefficients	Denominator coefficients
3rd	Proposed	$0.13413,\ 1.09438,\ -1.09438,\ -0.13413$	$1,\ 0.30329,\ -0.08539$
	Barsainya et al. [15]	$0.53177,\ 0.8672,\ -0.8672,\ -0.53177$	$1,\ 1.1022,\ 0.34957,\ 0.02675$
	Gupta et al. [8]	$1,\ -1,\ 0,\ 0$	$0.87608,\ 0.14690,\ -0.03458,\ 0.01269$
	Al-Alaoui and Baydoun [10]	$1.1533,\ -0.4432,\ -0.706,\ -0.0041$	$1,\ 0.7981,\ 0.0884,\ 0$
	Nongpiur et al., example 3 [12]	$-0.0895,\ 1.1668,\ -0.0889,\ -0.9883$	$1,\ 0.9714,\ 0.0782,\ -0.0104$
5th	Proposed	$-0.07838,\ 0.09957,\ 1.09359,$ $-1.09359,\ -0.09957,\ 0.07838$	$1,\ 0.30379,$ $-0.06339,\ 0.04990$
	Barsainya et al. [15]	$0.1295,\ 0.6828,\ 0.6019,$ $-0.6019,\ -0.6828,\ -0.1295$	$0.6541,\ 1.3175,\ 0.9691,$ $0.3156,\ 0.0435,\ 0.0018$
	Devate et al. [13]	$0.25,\ 2.1408,\ 2.0522,$ $-2.0523,\ -2.1407,\ -0.2499$	$2.2257,\ 4.1683,\ 2.63,$ $0.6353,\ 0.0517,\ 0$

Table 3: Number of multiplications required by the proposed and existing recursive fullband differentiators, maximum absolute magnitude and phase response errors.

Order	Reference	No. of multipliers	Max. mag. error	Max. phase error, rad
3rd	Proposed	3	0.1043	0.3684
	Barsainya et al. [15]	4	0.0993	1.1389
	Gupta et al. [8]	4	0.2071	0.1895
	Al-Alaoui and Baydoun [10]	6	0.0584	0.1799
	Nongpiur et al., example 3 [12]	6	0.0959	0.0550
5th	Proposed	4	0.0757	0.3677
	Barsainya et al. [15]	6	0.0835	2.1001
	Devate et al. [13]	11	0.0293	1.9818

with the 3rd order low-pass filter $Q_3(z)$ having a passband edge frequency equal to $\omega_p = 0.5\pi$ are shown in Figs. 12 and 13. As expected, the low-pass differentiator $G\left(z,\, \mathbf{W}^{(2)}\right) = H\left(z,\, \mathbf{W}^{(2)}\right) Q_3(z)$ exhibits a lower absolute magnitude response and phase response linearity errors in the passband compared to low-pass differentiator $G\left(z,\, \mathbf{W}^{(1)}\right) = H\left(z,\, \mathbf{W}^{(1)}\right) Q_3(z)$, due to different weighting factors utilized in the corresponding fullband differentiator design. Namely, in case of fullband differentiator $H\left(z,\, \mathbf{W}^{(2)}\right)$, the choice of weighting factors allows the passband magnitude response error minimization which is, at some extent, followed by the phase response linearity improvement.

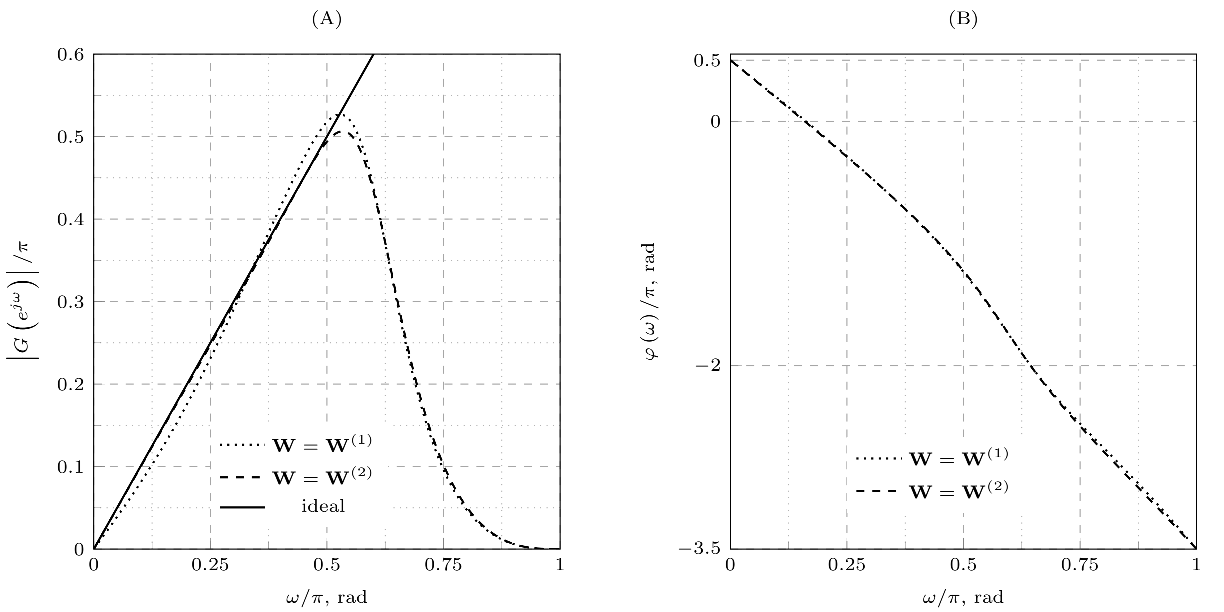

Figure 12: (A) Magnitude and (B) phase responses of the IIR low-pass differentiators $G\left(z,\, \mathbf{W}^{(1)}\right)$ and $G\left(z,\, \mathbf{W}^{(2)}\right)$.

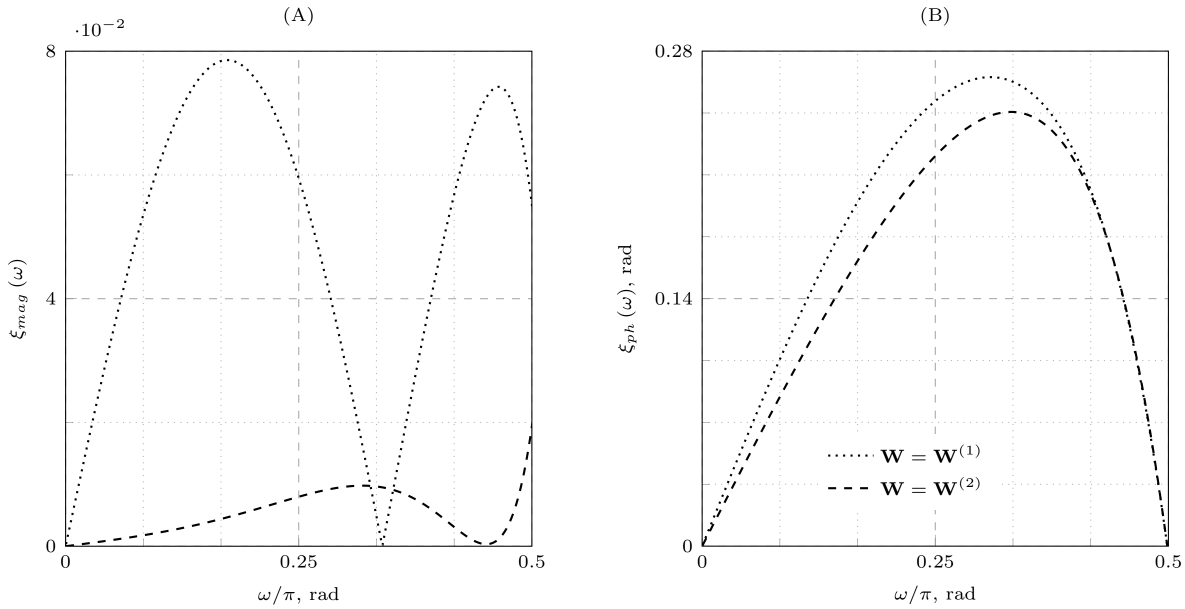

Figure 13: (A) Absolute magnitude response error functions and (B) phase response linearity error functions of the low-pass differentiators $G\left(z,\, \mathbf{W}^{(1)}\right)$ and $G\left(z,\, \mathbf{W}^{(2)}\right)$.

The absolute magnitude response error function and the phase response linearity error function of the low-pass differentiators obtained by cascading 7th order proposed IIR fullband differentiator $H\left(z,\, \mathbf{W}^{(3)}\right)$, where

$$\mathbf{W}^{(3)} = [100,\, 100,\, 100,\, 100,\, 1]\,, \tag{42}$$

with 1st, 2nd and 3rd order low-pass filter $Q_L(z)$ with the passband edge frequency $\omega_p = 0.35\pi$, are given in Fig. 14. As can be observed, low-pass differentiator's phase response linearity is primarily affected by the nonlinearity of the corresponding Chebyshev I low-pass filter's phase response, Fig. 14B, while better suppression of the high frequency noise is achieved if the order of the low-pass filter L is higher, Fig. 15A. Therefore, a compromise should be made between the phase response linearity error of the proposed low-pass differentiators and their selectivity in the stopband if the Chebyshev I low-pass filter (or any other IIR low-pass filter type) is used. Phase responses of obtained low-pass differentiators are given in Fig. 15B.

Regarding the convergence behavior of the proposed algorithm when weighting factors are equal to

$$W_k = \begin{cases} 100, & k \leq N \\ 1, & k = N+1 \end{cases}, \tag{43}$$

for N from 1 to 40, fast convergence is observed. Namely, it shows that required number of iterations is less than or equal to 7 for each N from 1 to 40 and $\Delta_{tol} = 10^{-10}$.

4.2.1. Comparison with existing low-pass differentiators

Low-pass differentiators obtained by cascading second order Chebyshev I low-pass filter $Q_2(z)$ with the proposed third order IIR fullband differentiator characterized by the weighting factors' vector $\mathbf{W}^{(2)}$, Eq. 41, are compared to IIR low-pass differentiators of the 5th order from [24]. Magnitude and phase responses of those differentiators and the corresponding error functions are presented in Figs. 16 and 17, respectively. As can be observed in Fig. 16A, 5th order low-pass differentiators from [24] exhibit better suppression of the high frequency noise compared to the low-pass differentiators obtained by cascading proposed fullband differentiator with Chebyshev I low-pass filters. On the other hand, the absolute magnitude response errors, Fig. 17A, and especially the phase linearity errors, Fig. 17B, are considerably lower in case of proposed low-pass differentiators.

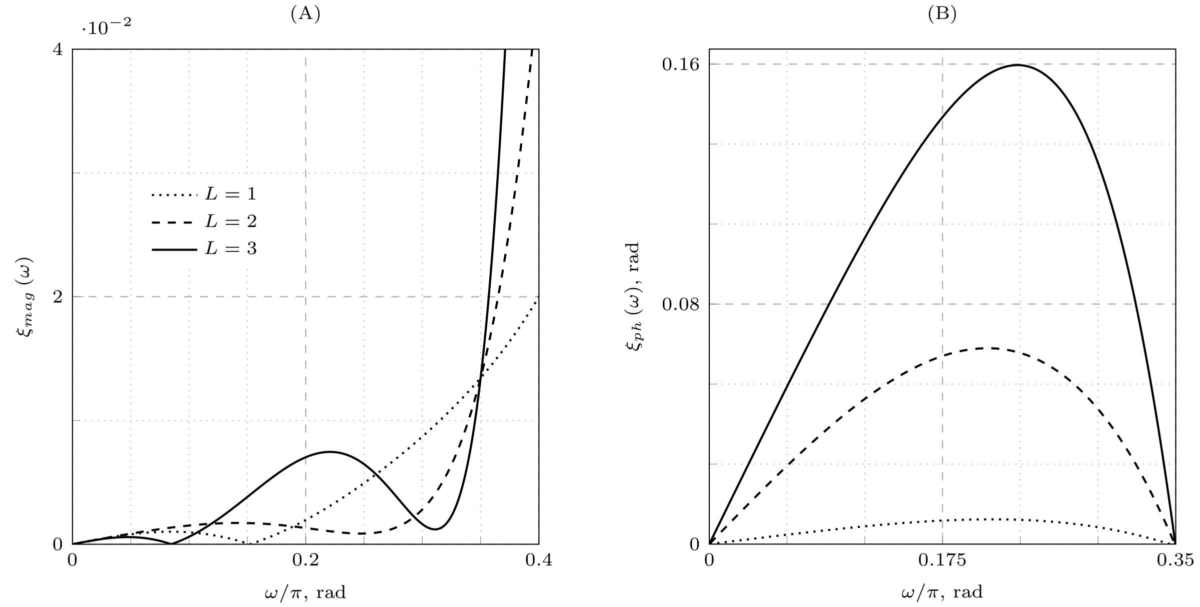

Figure 14: (A) Absolute magnitude response error function and (B) phase linearity error function of the low-pass differentiator obtained by cascading the proposed fullband differentiator $H\left(z,\, \mathbf{W}^{(3)}\right)$ with the low-pass filter $Q_L(z)$ for $L = 1,\, 2,\, 3$.

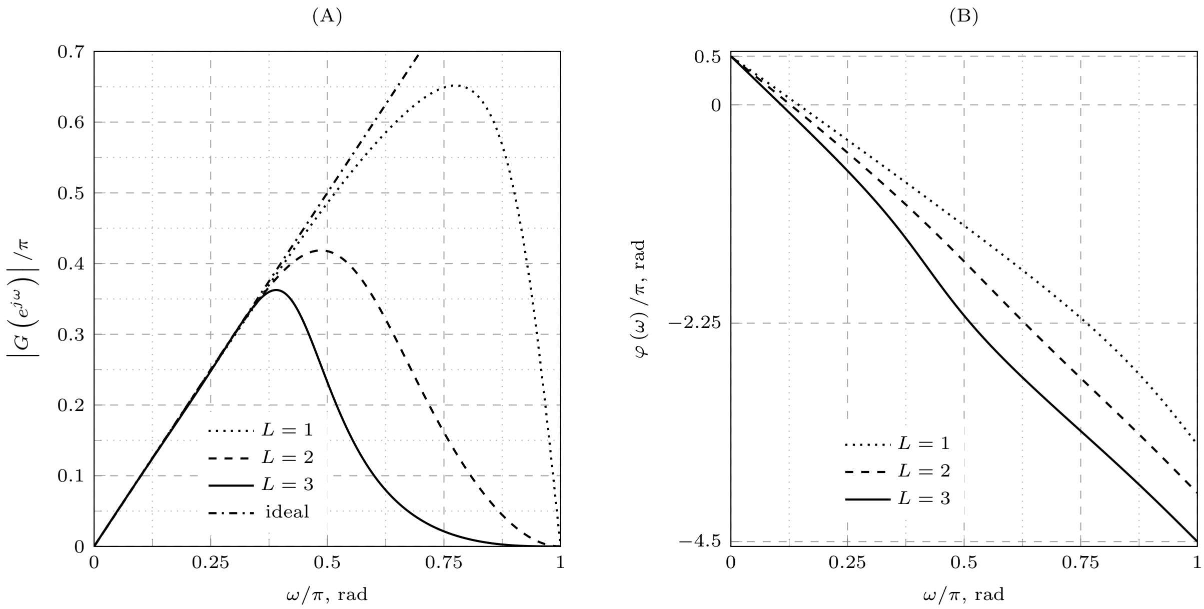

Figure 15: (A) Magnitude and (B) phase responses of the low-pass differentiator obtained by cascading the proposed fullband differentiator $H\left(z,\, \mathbf{W}^{(3)}\right)$ with the low-pass filter $Q_L(z)$ for $L = 1,\, 2,\, 3$.

The coefficients of the considered 5th order low-pass differentiators are given in Tab. 4, while the needed number of multiplications required by those differentiators are given in Tab. 5.

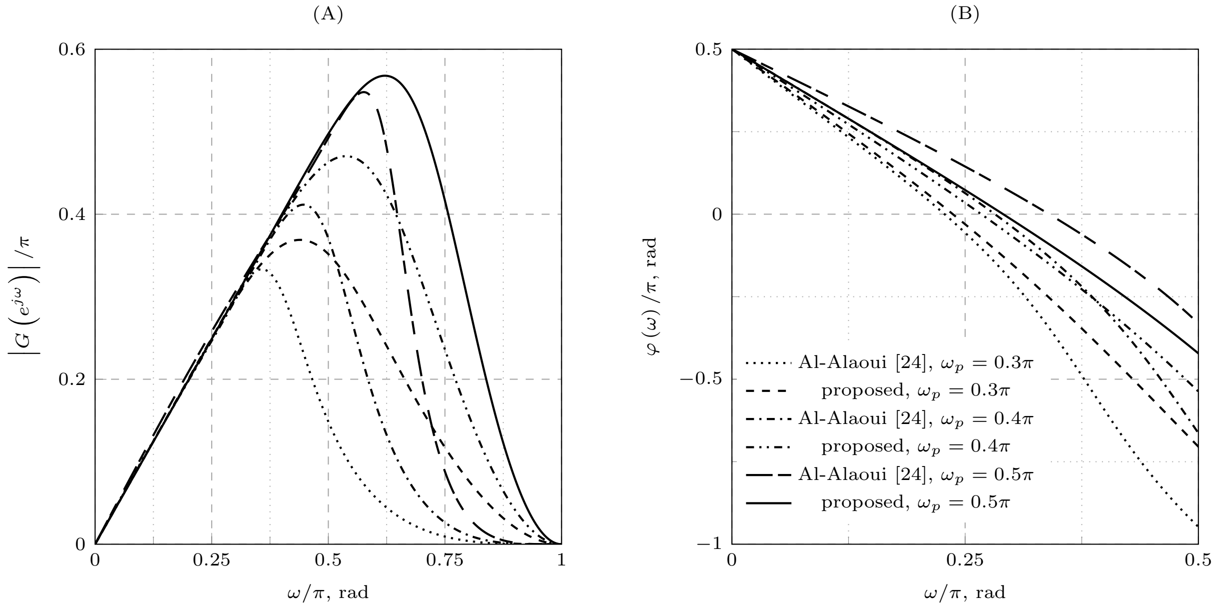

Figure 16: (A) Magnitude and (B) phase responses of the proposed and existing low-pass differentiators of the 5th order.

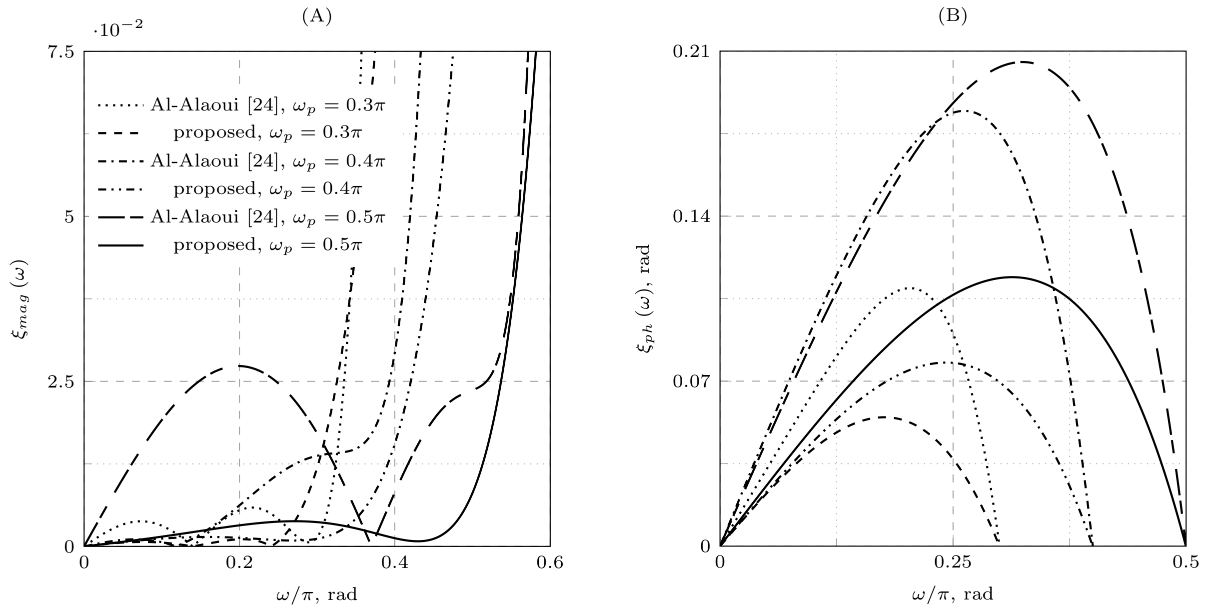

Figure 17: (A) Absolute magnitude response error functions and (B) phase linearity error functions of the proposed and existing low-pass differentiators of the 5th order.

5. Conclusion

Although the proposed IIR fullband differentiator design method does not result in transfer function having linear (or nearly-linear) phase response, nor the phase response linearity error can be controlled for $\omega \in (0, \pi)$, it yields lower phase response linearity error compared to some of the existing IIR fullband differentiators. On the other hand, the magnitude response error can be controlled by varying the order of the corresponding all-pass filter $A_N(z)$. To facilitate the determination of the needed order of the all-pass filter,

Table 4: Coefficients of the 5th order low-pass differentiators from [24] and low-pass differentiators of the same order obtained by cascading 3rd order proposed fullband differentiator with 2nd order Chebyshev I low-pass filters.

ω_p	Reference	Numerator coefficients	Denominator coefficients
0.3π	Proposed	$0.0101,\ 0.3379,\ 0.3278,$ $-0.3278,\ -0.3379,\ -0.0101$	$1,\ 0.1791,\ 0.1645,$ $0.0594,\ -0.0049$
	Al-Alaoui [24]	$0.066,\ 0.198,\ 0.132,$ $-0.132,\ -0.198,\ -0.066$	$1,\ -0.3332,\ 0.3041,$ $0.1178,\ -0.0454,\ -0.0137$
0.4π	Proposed	$0.0141,\ 0.4714,\ 0.4573,$ $-0.4573,\ -0.4714,\ -0.0141$	$1,\ 0.6052,\ 0.2966,$ $0.0541,\ -0.0053$
	Al-Alaoui [24]	$0.1178,\ 0.3534,\ 0.2356,$ $-0.2356,\ -0.3534,\ -0.1178$	$1,\ 0.3021,\ 0.4396,$ $0.143,\ -0.0093,\ -0.0053$
0.5π	Proposed	$0.0178,\ 0.5974,\ 0.5795,$ $-0.5795,\ -0.5974,\ -0.0178$	$1,\ 0.9623,\ 0.4541,$ $0.0623,\ -0.0067$
	Al-Alaoui [24]	$0.2032,\ 0.6096,\ 0.4064,$ $-0.4064,\ -0.6096,\ -0.2032$	$1,\ 0.9515,\ 0.8383,$ $0.2321, 0.0255, -0.0004$

Table 5: Number of multiplications required by the 5th order low-pass differentiators from [24] and low-pass differentiators of the same order obtained by cascading 3rd order proposed fullband differentiator with 2nd order Chebyshev I low-pass filters, maximum absolute magnitude and phase response errors.

ω_p	Reference	No. of multipliers	Max. mag. error	Max. phase error, rad
0.3π	Proposed	5	0.0119	0.0547
	Al-Alaoui [24]	6	0.0059	0.1094
0.4π	Proposed	5	0.0154	0.0779
	Al-Alaoui [24]	6	0.0291	0.1846
0.5π	Proposed	5	0.0080	0.1141
	Al-Alaoui [24]	6	0.0273	0.2054

characterizing the IIR fullband differentiator with equiripple magnitude response such that its maximum magnitude error is less than or equal to some prescribed value, the inequality given by Eq. 39 is derived. The results of fullband differentiators' comparison imply that the proposed IIR fullband differentiators require less multiplications compared to the existing fullband differentiators.

Since the phase response of the proposed IIR fullband differentiators is nearly-linear function of frequency for ω small, IIR low-pass differentiators obtained by the cascading approach are also considered. It is shown that the passband magnitude response error of such low-pass differentiators can be decreased by an appropriate choice of the weighting factors' vector for the corresponding proposed IIR fullband differentiators design. Furthermore, this improvement of the passband magnitude response is followed by the improvement of the passband phase response of the low-pass differentiator. Obtained IIR low-pass differentiators, apart from requiring the less number of multiplications, exhibit lower passband magnitude response error and the lower phase response linearity error compared to some of the existing low-pass differentiators of the same order.

Acknowledgments

This work was supported by the Ministry of Education, Science and Technological Development of the Republic of Serbia under the project TR33035.

References

[1] M. A. Al-Alaoui, Direct approach to image edge detection using differentiators, in: Electronics, Circuits, and Systems (ICECS), 2010 17th IEEE International Conference on, IEEE, 2010, pp. 154–157.

[2] Y. Xu, T. Dai, K. Sycara, M. Lewis, Service level differentiation in multi-robots control, in: Intelligent Robots and Systems (IROS), 2010 IEEE/RSJ International Conference on, IEEE, 2010, pp. 2224–2230.

[3] G. F. Franklin, J. D. Powell, M. L. Workman, Digital control of dynamic systems, Vol. 3, Addison-wesley Menlo Park, CA, 1998.

[4] C. Nayak, S. K. Saha, R. Kar, D. Mandal, An Efficient QRS Complex Detection Using Optimally Designed Digital Differentiator, Circuits, Systems, and Signal Processing (2018) 1–34doi:10.1007/s00034-018-0880-y.

[5] Z. Xin, X. Wang, P. C. Loh, F. Blaabjerg, Realization of Digital Differentiator Using Generalized Integrator For Power Converters, IEEE Transactions on Power Electronics 30 (12) (2015) 6520–6523. doi:10.1109/TPEL.2015.2442414.

[6] M. A. Al-Alaoui, Novel approach to designing digital differentiators, Electronics Letters 28 (15) (1992) 1376–1378. doi:10.1049/el:19920875.

[7] N. Q. Ngo, A new approach for the design of wideband digital integrator and differentiator, IEEE Transactions on Circuits and Systems II: Express Briefs 53 (9) (2006) 936–940. doi:10.1109/TCSII.2006.881806.

[8] M. Gupta, M. Jain, B. Kumar, Recursive wideband digital integrator and differentiator, International Journal of Circuit Theory and Applications 39 (7) (2011) 775–782.

[9] M. Jain, M. Gupta, N. Jain, Linear phase second order recursive digital integrators and differentiators, Radioengineering 21 (2) (2012) 712–717.

[10] M. A. Al-Alaoui, M. Baydoun, Novel wide band digital differentiators and integrators using different optimization techniques, in: Signals, Circuits and Systems (ISSCS), 2013 International Symposium on, IEEE, 2013, pp. 1–4.

[11] M. Gupta, B. Relan, R. Yadav, V. Aggarwal, Wideband digital integrators and differentiators designed using particle swarm optimisation, IET Signal Processing 8 (6) (2014) 668–679.

[12] R. C. Nongpiur, D. J. Shpak, A. Antoniou, Design of IIR digital differentiators using constrained optimization., IEEE Trans. Signal Processing 62 (7) (2014) 1729–1739.

[13] J. Devate, S. Kulkarni, K. Pai, Wideband IIR digital integrator and differentiator using curve fitting technique, in: Signal Processing, Communication and Networking (ICSCN), 2015 3rd International Conference on, IEEE, 2015, pp. 1–4.

[14] M. Kumar, T. K. Rawat, A. Jain, A. A. Singh, A. Mittal, Design of digital differentiators using interior search algorithm, Procedia Computer Science 57 (2015) 368–376.

[15] R. Barsainya, T. K. Rawat, Novel design of recursive differentiator based on lattice wave digital filter, Radioengineering 26 (1) (2017) 387–395.

[16] M. K. Jalloul, M. A. Al-Alaoui, Design of recursive digital integrators and differentiators using particle swarm optimization, International Journal of Circuit Theory and Applications 44 (5) (2016) 948–967. doi:10.1002/cta.2115.

[17] S. Mahata, S. K. Saha, R. Kar, D. Mandal, Optimal design of wideband digital integrators and differentiators using harmony search algorithm, International Journal of Numerical Modelling: Electronic Networks, Devices and Fields 30 (5) (2017) e2203, e2203 JNM-15-0191.R1. doi:10.1002/jnm.2203.

[18] C.-C. Tseng, Stable IIR digital differentiator design using iterative quadratic programming approach, Signal Processing 80 (5) (2000) 857–866.

[19] X. Lai, Z. Lin, Iterative Reweighted Minimax Phase Error Designs of IIR Digital Filters With Nearly Linear Phases, IEEE Transactions on Signal Processing 64 (9) (2016) 2416–2428. doi:10.1109/TSP.2016.2521610.

[20] M. Nakamoto, S. Ohno, Design of Multi-Band Digital Filters and Full-Band Digital Differentiators Without Frequency Sampling and Iterative Optimization, IEEE Transactions on Industrial Electronics 61 (9) (2014) 4857–4866. doi:10.1109/TIE.2013.2290765.

[21] P. N. Lekić, A. D. Micić, Direct synthesis of the digital FIR full-band differentiators, Facta universitatis-series: Electronics and Energetics 15 (3) (2002) 465–479.

[22] I. W. Selesnick, Maximally flat low-pass digital differentiator, IEEE Transactions on Circuits and Systems II: Analog and Digital Signal Processing 49 (3) (2002) 219–223.

[23] Z. U. Sheikh, H. Johansson, A Class of Wide-Band Linear-Phase FIR Differentiators Using a Two-Rate Approach and the Frequency-Response Masking Technique, IEEE Transactions on Circuits and Systems I: Regular Papers 58 (8) (2011) 1827–1839. doi:10.1109/TCSI.2011.2107270.

[24] M. A. Al-Alaoui, Linear phase low-pass IIR digital differentiators, IEEE Transactions on signal processing 55 (2) (2007) 697–706.